Microwave-Plasma-Coupled Re-Ignition of Methane-and-Oxygen Mixture Under Auto-Ignition Temperature

Xing Rao, Stephen Hammack, Campbell Carter, Timothy Grotjohn, Jes Asmussen, Jr., *Life Fellow, IEEE*, and Tonghun Lee

***Abstract*—The re-ignition phenomenon is observed when fuel/oxidizer is re-introduced into an atmospheric-pressure plasma discharge generated by cutting off the gas flow in a re-entrant microwave-plasma applicator system used for plasma-assisted ignition and combustion research works. Results indicate that, for re-ignition to occur, the electric field must be strong enough to fully establish a weakly ionized and self-sustained plasma discharge, and with elevated radical concentrations. The re-ignition was possible at gas flow speeds higher than typical flame propagation rates, and temperature measurements (thermocouple and N_2 emission) reveal that re-ignition occurs under auto-ignition temperatures. The high-speed imaging of the flame propagation shows that it is a two step process of initiating a fast pyrolysis flame, which, in turn, stabilizes and starts the direct coupling process of the plasma energy into the flame for full re-ignition to occur.**

***Index Terms*—Auto-ignition temperature, laser induced fluorescence, plasma assisted combustion, re-ignition.**

I. Introduction

PLASMA-ASSISTED combustion and ignition are believed to be promising technologies that can enable highly efficient thermal energy conversion and stable ignition under practical and harsh environments [1], [2]. Combining electromagnetic radiation with thermal oxidation leads to faster and more intense chemical energy conversion, increased stability in the lean flammability limit, improved fuel efficiency through more complete combustion, reduction of pollution by altering oxidation by-products, stable fuel oxidation across a broader range of pressures and temperatures, and more reliable and rapid ignition [3]–[8]. It is also particularly promising in the development of next-generation hypersonic propulsion systems in which the ignition of the high-speed gases is a critical issue to be resolved [3], [8].

Manuscript received February 25, 2011; revised May 24, 2011; accepted June 16, 2011. Date of publication August 4, 2011; date of current version December 14, 2011. This work was supported by the Air Force Office of Scientific Research under Award FA9550-09-1-0282 and Award FA9550-10-1-0556 with Dr. J. Tishkoff as Technical Monitor.

X. Rao is with the Facility for Rare Isotope Beam, Michigan State University, East Lansing, MI 48824 USA.

S. Hammack and T. Lee are with the Department of Mechanical Engineering, Michigan State University, East Lansing, MI 48824 USA.

C. Carter is with the Air Force Research Laboratory, Wright-Patterson AFB, OH 45433 USA.

T. Grotjohn and J. Asmussen, Jr. are with the Department of Electrical and Computer Engineering, Michigan State University, East Lansing, MI 48824 USA.

Digital Object Identifier 10.1109/TPS.2011.2161597

Currently, various research groups are working on the exact mechanism for flame and ignition enhancement by a plasma discharge and have provided insights into various aspects of this complicated process [9]–[14]. It appears that the electromagnetic energy alters the reaction chemistry by the following: 1) the decomposition of the fuel from larger to smaller hydrocarbons and the creation of radicals via collision with electrons; 2) the radiation-induced electron excitation; 3) the increased flame temperature by ohmic heating; 4) the increase in excited-state species, ions, and electrons; and 5) the *in situ* fuel reformation. A large number of different discharge systems including microwave, direct current, radio frequency, etc., have been investigated by various research groups [9]–[17] using both experimental and numerical approaches. The mechanism of plasma-assisted ignition has been also intensively investigated with several possible mechanisms proposed such as localized ohmic heating, catalytic NO_X enhancement, and nonequilibrium dissociation and excitation of oxygen and fuel [1], [18], [19]. Many of the studies of plasma-assisted ignition have been devoted to the use of a high-voltage nanosecond discharge below self-ignition threshold, which shows that the enhancement is primarily associated with kinetic mechanisms from O and H atoms dissociated by the plasma [20]–[22].

In our previous work, we have looked into an efficient plasma enhancement concept where the plasma energy is directly coupled into the reaction zone [16], [23], enabling the ionization to occur at very low power levels. The electric field interacts with the ions and the electrons already present in the flame to initiate a plasma discharge, which, in turn, accelerates the combustion chemistry. As the plasma is sustained by the pilot flame in this case, what happens when the pilot flame is extinguished and re-ignition is required? This paper is an extension of that effort to investigate the re-ignition conditions that are required in this type of concept. Here, we study the conditions where the plasma discharge is self-sustained in the event that the pilot flame is extinguished using laser and optical diagnostics to identify the radical concentrations and the thermodynamic state. Once the plasma is established, it will act as the re-ignition source, and the conditions of the plasma plume are once again characterized using optical measurements. The term "re-ignition" in this paper refers to the ignition of premixed flow re-introduced to the plasma zone after the flame has been extinguished. The interval time is on the order of more than 10 s to make sure that the remaining unstable and/or

Report Documentation Page

Form Approved
OMB No. 0704-0188

1. REPORT DATE	2. REPORT TYPE	3. DATES COVERED
14 DEC 2011		**00-00-2011 to 00-00-2011**

4. TITLE AND SUBTITLE	5a. CONTRACT NUMBER
Microwave-Plasma-Coupled Re-Ignition of Methane-and-Oxygen Mixture Under Auto-Ignition Temperature	5b. GRANT NUMBER
	5c. PROGRAM ELEMENT NUMBER
6. AUTHOR(S)	5d. PROJECT NUMBER
	5e. TASK NUMBER
	5f. WORK UNIT NUMBER
7. PERFORMING ORGANIZATION NAME(S) AND ADDRESS(ES) **Michigan State University,Department of Mechanical Engineering,East Lansing,MI,48824**	8. PERFORMING ORGANIZATION REPORT NUMBER
9. SPONSORING/MONITORING AGENCY NAME(S) AND ADDRESS(ES)	10. SPONSOR/MONITOR'S ACRONYM(S)
	11. SPONSOR/MONITOR'S REPORT NUMBER(S)

12. DISTRIBUTION/AVAILABILITY STATEMENT
Approved for public release; distribution unlimited

13. SUPPLEMENTARY NOTES

14. ABSTRACT

The re-ignition phenomenon is observed when fuel/ oxidizer is re-introduced into an atmospheric-pressure plasma discharge generated by cutting off the gas flow in a re-entrant microwave-plasma applicator system used for plasma-assisted ignition and combustion research works. Results indicate that, for re-ignition to occur, the electric field must be strong enough to fully establish a weakly ionized and self-sustained plasma discharge and with elevated radical concentrations. The re-ignition was possible at gas flow speeds higher than typical flame propagation rates, and temperature measurements (thermocouple and N2 emission) reveal that re-ignition occurs under auto-ignition temperatures. The high-speed imaging of the flame propagation shows that it is a two step process of initiating a fast pyrolysis flame, which, in turn, stabilizes and starts the direct coupling process of the plasma energy into the flame for full re-ignition to occur.

15. SUBJECT TERMS

16. SECURITY CLASSIFICATION OF:			17. LIMITATION OF ABSTRACT	18. NUMBER OF PAGES	19a. NAME OF RESPONSIBLE PERSON
a. REPORT	b. ABSTRACT	c. THIS PAGE			
unclassified	**unclassified**	**unclassified**	**Same as Report (SAR)**	**7**	

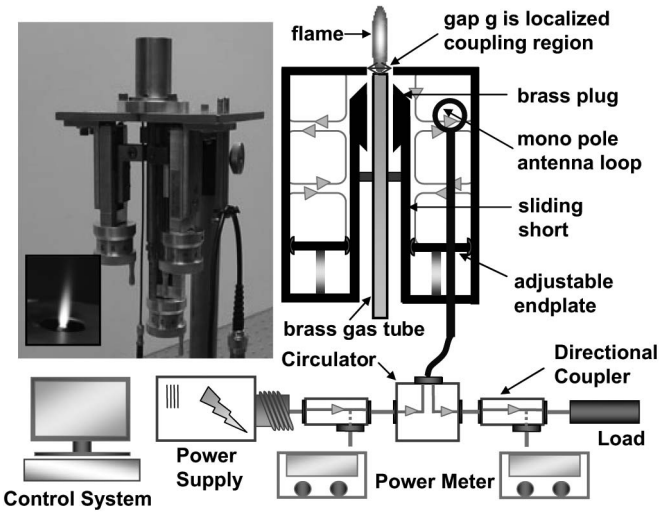

Fig. 1. Diagram of re-entrant microwave-plasma cavity and combustion system.

excited-state species generated by the previous fuel–oxidizer mixture do not affect the re-ignition process. Flame propagation during the re-ignition process, as a function of reactant flow rate, has been also investigated. The re-ignition phenomena, which can occur in this highly efficient direct-coupled microwave-plasma-enhanced combustion system, can provide a fundamental understanding of the relevant chemistry and thermodynamic influences and will contribute to the use of such concepts for practical systems in the future.

II. Experimental Setup

A. Microwave Re-Entrant Cavity Applicator

The coaxial re-entrant cavity applicator used in this paper was previously introduced [23], [24], and only a brief description will be given here. The torch was developed for coupling microwave energy directly into the reaction zone. The "direct plasma coupling" concept offers the advantage of efficient plasma initiation and stabilization at relatively low plasma power.

Fig. 1 shows a photo and a schematic of this microwave-plasma applicator. The 2.45-GHz microwave energy is transmitted via a coaxial cable and emitted with a monopole antenna loop. When the relative location of the torch, the antenna, and the baseplate are adjusted using the unislides, an optimized resonant mode can be found, where most of the energy is focused into the region between the edge of the outer cavity and the end of the combustion torch. There are several nearby operating modes that can be accessed by changing the combination of the three-way adjustments. We select a mode that allows the center torch to be exposed outside the main chamber, so that the flame is clearly visible and can accommodate laser and optical diagnostics. The chamber itself is 35 mm in diameter and is generally optimized to a length of around 3 cm ($\lambda/4$ for 2.45 GHz). The chamber is constructed of brass, which can be considered a perfect electrical conductor for practical purposes. The small insert on the left side shows a photo of the flame with 20-standard-cm^3/min (SCCM) methane and 40-SCCM oxygen. Here, standard conditions refer to a temperature of 273.15 K and a pressure of 101.325 kPa.

In the lower half of Fig. 1, the setup and the components for the microwave power supply, and the measurement system are shown. It consists of a power supply, two directional couplers, two power meters with a power sensor, and a circulator. Two directional couplers and two power meters are used because both the incident power and the reflected power have to be measured and calibrated. This system is used to select the exact resonant modes and monitor the absorbed power that is coupled into the plasma applicator system.

B. Diagnostic Methods

Several optical diagnostic methods were used in this paper, including laser-induced fluorescence [hydroxyl (OH), carbon monoxide (CO), and atomic oxygen (O)], emission measurements (OH and N_2 emissions), and high-speed photography (a frame rate of 10 kHz).

The excitation of OH was made using the $Q_1(8)$ transition from the $A^2\Sigma^+ - X^2\prod$ (1,0) [25] band, which requires narrow-band ultraviolet light near 283 nm. The measurements were conducted using a dye laser (Lumonics Hyperdye HD-300) with the output of 7-ns pulses at 566 nm, which was subsequently frequency doubled through an Inrad Autotracker (ATIII) to a final frequency of 283 nm. The laser is pulsed at 10 Hz with a spectral linewidth of about 0.1 cm^{-1} at 283 nm. The pulse energy, typically 8 mJ per pulse, was digitally recorded using a fast photodiode and an oscilloscope. The laser was expanded into a sheet, and the fluorescence signal was collected at 90° using an intensified charge-coupled-device (CCD) camera with a WG305 filter. A flat flame test burner was used for the calibration of the laser wavelength, and a Hencken burner was used to correlate the signal intensity with the actual OH number density.

CO in the reaction zone was measured using two-photon planar laser-induced fluorescence (LIF), pumping the $B^1\Sigma^+ - X^1\Sigma^+$ (0,0) transition at 230.10 nm [26]. The measurements are based on assumptions made that the rate of photoionization is higher than that of quenching and predissociation [27] and that the interference of C_2 by laser photodissociation is minimal using our filter selection [26]. The correction for pulse-to-pulse fluctuations is important due to the sensitivity with the LIF signal and was taken into consideration for all the cases. The emission spectrum of CO reaches maximum at 230.10 nm. The 532-nm beam from a Newport Nd:YAG was used to pump a Sirah Precisionscan LG-2400 dye laser operating with Exciton DCM dye. The 653-nm output of the dye laser was sum-frequency-mixed with the third harmonic beam (355 nm) from the injection-seeded Nd:YAG laser to produce 230-nm radiation (linewidth ~ 0.1 cm^{-1}) needed for the two-photon LIF. The pulse energy is digitally recorded using an energy monitor from LaVision.

Atomic-oxygen LIF was achieved using ~226-nm laser light, with a transition of $3p^3P - 2p^3P$, after which the molecules are transition to a $3s^3$ state while emitting fluorescence light at 844.87 nm. The experiment pressure (1 bar) results in a nonnegligible collisional quenching and a subsequent decrease in fluorescence quantum [28]. Due to the complexity of all the

spectroscopic and optical parameters related to the observed LIF signal and photolytic and multiphoton effects with O_2 and CO_2, the relative signal intensity will be presented here for a first-order qualitative comparison. The measurements were conducted using a dye laser (Sirah Precisionscan-LG-2400) with two-stage amplification. The 532-nm laser beam was used to pump a dye laser and is then sum-frequency mixed with 355 nm (third harmonic) of Nd:YAG to a final output frequency of 226.03 nm. Laser pulse energy ranged from $10 \sim 13$ mJ per pulse with a 7-ns pulse duration. The laser is pulsed at 10 Hz with a final linewidth of 0.2 cm^{-1} at 226.03 nm.

The OH emission spectrum is used to calculate the OH rotational temperature in the plasma-assisted combustion reaction zone using a 0.033-nm resolution scan over emission between 307 and 308 nm. As the signal is from chemically excited species, the emission intensity is a relative measure of concentration. For the reported temperatures, the OH population of individual energy states is assumed to follow a Boltzmann distribution, and the rotational thermometry is carried out by using four transitions [$R_2(14)$ (307.1145 nm), $R_2(15)$ (307.3028 nm), $R_2(4)$ (307.4369 nm), and $R_2(3)$ (307.7028 nm)] [29].

In an atmospheric air discharge, the OH rotational thermometry is not feasible due to the lack of hydrogen. In this case, we used emission from the second positive system of molecular nitrogen ($C^3\prod - B^3\prod, \Delta v = 2$). This transition is used due to its signal intensity and its clearly resolved individual vibrational bands. Moreover, these emission lines between 365 and 385 nm are far from other air emission lines, and thus, there is less interference. The measured spectrum was compared with numerically generated spectra for both the rotational and vibrational temperatures [30]. Here, it is assumed that the rotational and vibrational temperatures are in partial equilibrium, the upper energy level is in nonequilibrium between the vibrational and rotational modes, and every internal energy mode forms an equilibrium state based on the Boltzmann distribution function. For comparison, thermocouple measurements have also been made using a probe bead of 0.02 in diameter. It is acknowledged that the thermocouple will interfere with the discharge; however, the temperatures are collected at the tip of the discharge to minimize this effect, and the resulting temperatures provide valuable estimation of the rough thermodynamic conditions in the plasma discharge.

Photographic images of the air microwave discharge were taken using a standard CCD camera, while the re-ignition process and the flame evolution were recorded with a high-speed camera Photron FASTCAM SA5 with high frame rates up to 10 kHz.

III. Results and Discussion

A. Microwave-Discharge-Assisted Combustion of Methane/Oxygen

The first important issue is to understand under what conditions the plasma is able to self-sustain (and enable re-ignition) if the pilot flame is extinguished. Images of the pilot flame and the microwave interaction using methane and oxygen are shown in Fig. 2. It is clearly shown that three distinct stages are observed, depending on the input microwave power. In Stage I, termed the "electric-field-enhanced stage," the microwave energy is low,

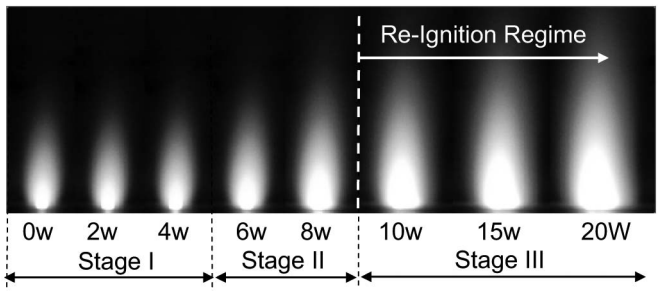

Fig. 2. Images of CH_4/O_2 flame versus microwave power with three stages of plasma coupling (100-SCCM total flow rate at $\phi = 1.1$).

and only a small amount of microwave energy is coupled into the flame, but no microwave plasma is produced. The flame does not visually change while the flammability and the flame speed are increased, and slight increases in temperature due to ohmic heating and *in situ* fuel reforming are observed [23]. As the microwave power increases between 6 and 10 W, shown in the figure as Stage II, i.e., the "transition stage," a plasma plume is initiated. As the microwave power is increased further over 10 W and into Stage III, i.e., the "full plasma stage," the reaction zone is overlapped and dominated by a full plasma plume. We have found that the plasma will self-sustain after the flame (fuel and oxygen) is shut off when the microwave power is higher than 10 W and a weakly ionized discharge is fully developed in Stage III. The plasma can subsequently re-ignite the flame when the gas mixture is put back into the system, and therefore, this range is shown in Fig. 2 as the "re-ignition regime." The atmospheric microwave air discharge and re-ignition process will be discussed in greater detail in the following sections.

To understand the conditions of the re-ignition regime that enables the plasma to be self-sufficient, quantitative measurements of key combustion radicals (OH, CO, and O) and temperature in the reaction zone were made and are presented in Fig. 3. The total flow rate for all these measurements is 60 SCCM with an equivalence ratio of $\phi = 1.0$ at a location 5 mm above the torch tip.

Shown in the upper portion of Fig. 3, the OH concentration in the first stage (0–6 W) does not noticeably increase when the measurement uncertainty is considered ($\sim$8%). There is insufficient microwave energy to generate a cascade of ionization leading to a plasma discharge. In the "transition stage," the electron temperature exceeds the gas temperature, leading to inelastic collisions for excitation, dissociation, and ionization to generate new species and eventually break down to initiate a plasma discharge. At the same time, the OH concentration dramatically increases with important reaction pathways, i.e., $H_2O + e^- \rightarrow e^- + H + OH$, $H_2O + O \rightarrow OH + OH$, and $H + O_2 \rightarrow OH + O$ [31]. When the microwave power is even higher in Stage III, the OH number density is relatively stable partly due to a higher volume despite a slightly higher energy coupling efficiency. This extra energy is required to sustain the ionization when the flame is extinguished.

Moreover, shown in the upper portion of Fig. 3, the CO number density is shown using a calibrated value from Chemkin simulations using GRI-mech 3.0 [32] with 1-D flame modeling of methane and oxygen. Overall, the CO number density increases with the microwave power. In Stage I, the

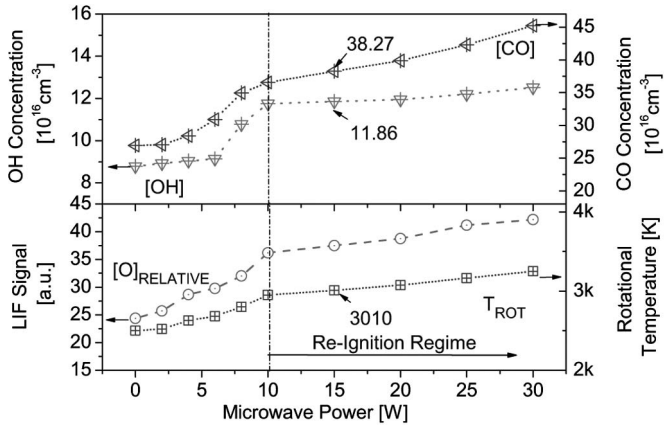

Fig. 3. Number density of OH and CO, relative O LIF signal intensity, and OH rotational temperature versus microwave power within the three stages of plasma coupling (60-SCCM total flow rate at $\phi = 1.1$).

in situ fuel reforming (to hydrogen and carbon monoxide), as well as the temperature increase, is expected to contribute to the enhancement in the flammability limits and the flame speed. Fuel reforming is observed from Stage I and is seen to dramatically increase through Stage II. Calculations show that, in our configuration, 18% of the total methane undergoes reforming to syngas at 30 W of microwave power, which is significant considering the competing oxidation reactions that subsequently lead to CO_2. The relative atomic oxygen (O) LIF signal and the OH rotational temperature are shown in the lower portion of Fig. 3. Atomic oxygen is monitored here mostly because it was reported as a critical role in the kinetics of plasma-enhanced flames [28] and also as a key radical in the self-sustainment of the plasma itself. The atomic-oxygen LIF emission increases with increased power similar to the trend of the other molecules with rapid propagation in Stage II, mainly from $O_2 + e \rightarrow O + O + e$ [33]. The OH rotational temperature increases over the whole power range of 10–30 W.

From the results, we find that the conditions for the plasma to self-sustain in the event of the pilot flame being extinguished is that the chemistry of the direct coupling is fully developed into a weakly ionized discharge and the excess energy is pumped into the system. At this stage, the radical concentrations have been also dramatically increased and almost maxed out. Below 10 W, the low temperature, degree of ionization, ionized volume, and electric-field strength fail to sustain the plasma discharge, and a general collapse of the combustion stabilization is expected.

B. Atmospheric Microwave Air Discharge

Once the flame is extinguished and the plasma discharge is self-sustained in atmospheric air, it needs to act as the ignition source for the fuel–air mixture. A set of images of this discharge (without flame) at different microwave power levels is shown in Fig. 4. The top row is taken from a side view, and the bottom row is taken by looking straight down onto the torch. In the top row, a white circle is marked to show the edge of the cavity. A first observation is that the size and the emission intensity increases with increased microwave power. Without the flame present, there is no dominant force to center the discharge, and

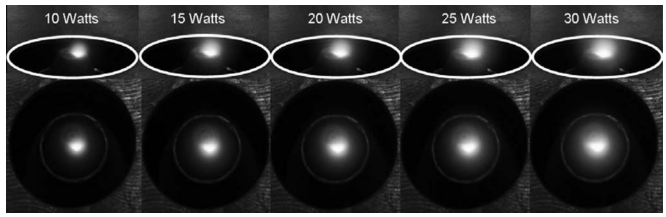

Fig. 4. Images of the microwave air discharge versus microwave power taken from (top row) the side and (bottom row) the top.

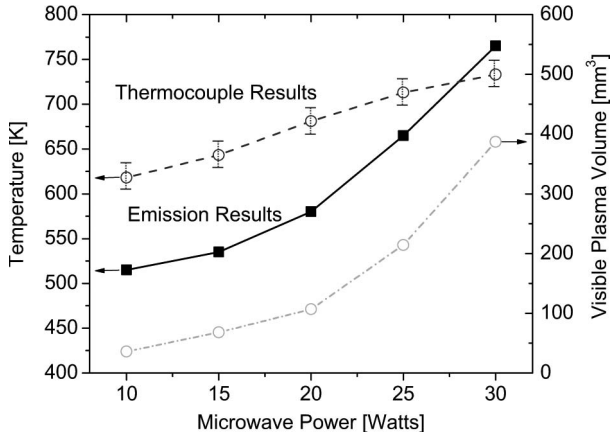

Fig. 5. Temperature (thermocouple and rotational N_2 emission) of the microwave air discharge with different power levels (left y-axis). Visible plasma volume with different power levels (right y-axis).

it wanders from side to side on the tip of the torch. In the air-discharge-only case shown in Fig. 4, the electric field is high enough to sustain this air discharge even without the excess heat and radicals from a pilot flame. The electron density is estimated to be around 10^{12-13} cm^{-3} in these conditions [34].

The parameters of these microwave discharges (thermocouple temperature, N_2 rotational temperature from emission, and plasma volume) are measured and shown in Fig. 5. The temperatures derived from both the thermocouple and the N_2 emission increase with higher microwave power in the same temperature range. It is interesting to note that all the measured temperatures are below the methane self-ignition temperature at atmospheric pressure, which is about 810 K [35], but the discharge is able to re-ignite the gas mixture when it is put back into the system. For all the temperatures measured from 10 to 30 W, the temperature ranges from 500 to 765 K using either thermocouple or N_2 rotational temperature measurements. However, this does not preclude the possibility of transient hotspots that can possibly contribute temperatures past the auto-ignition temperature for critical ignition volume. The ignition capacity in terms of input power will be discussed in the following section. Moreover, from Fig. 4, we can estimate a visible plasma volume assuming a spherical shape of the microwave air discharge. The slope of the plasma volume increase is greater at higher microwave power than at lower microwave power, due not only to the increase in ions and electrons but also to the increased mean free path at higher temperatures. We do note that, when we calculate the plasma power density from the ratio of microwave power over the visible discharge volume (intense center core), we get a decreased plasma power density with high power.

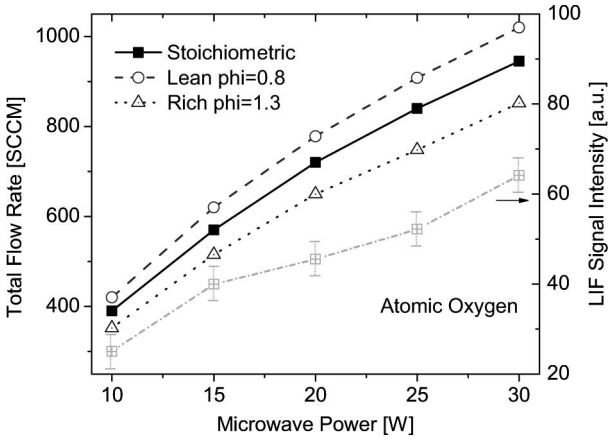

Fig. 6. Total flow rate limits with different microwave power levels for lean, stoichiometric, and rich conditions of re-introduced flow (left y-axis). Atomic-oxygen LIF signal intensity with different microwave power levels (right y-axis).

Nonetheless, the emission is stronger at higher powers, and the excited state radicals are expected to play a larger role in the re-ignition process.

C. Re-Ignition of Methane and Air Flow in the Microwave Discharge of Ambient Air Under Auto-Ignition Temperature

This section addresses the re-ignition process when the gases are reintroduced to the self-sustained plasma discharge. The addition of plasma has been shown to ignite different fuel–air mixtures below the auto-ignition threshold [22], and the same is observed here based on thermocouple measurements and emission spectroscopy. We have tried to quantify the re-ignition capacity of the plasma discharge with the microwave power between 10 and 30 W by increasing the reactant flow rate of the gas until we achieved blowoff. At each equivalence ratio and microwave power level, we increased the total reactant flow rate of the gas mixture, which is put back into the system until re-ignition could no longer be achieved. The results are plotted in Fig. 6 for different equivalence ratios (stoichiometric, rich, and lean). At the lowest microwave power shown here (10 W), the flow rate is about three times higher than the total flow rate limit possible to stabilize flame at the stoichiometric condition without any microwave power. The total flow rate limit without any microwave power is 100 SCCM.

It is clear from Fig. 6 that the total flow rate limits almost linearly increase with increased power. Moreover, the limits for the re-introduced fuel–lean mixture are the highest among the lean, stoichiometric, and rich ones, which agrees well with the theoretical understanding of minimum ignition energy as a function of equivalence ratio. To probe the reason for this dependence on the equivalence ratio and the power, the atomic-oxygen LIF was conducted in this region and presented in Fig. 6 (right y-axis). We estimate, in general, one order less of atomic oxygen in the microwave air discharge than that in the flame discussed in the previous sections based on the intensifier gain and the signal intensity. We can see a clear relationship between the atomic-oxygen LIF signal intensity and the total flow rate limits for different microwave power levels. The increase in atomic oxygen with higher microwave power (and lower equivalence ratios) can possibly explain the increase in total flow rate blowoff limits. It is believed that atomic oxygen helps ignition through reaction $O + CH_3 \rightarrow H + CH_2O$ as the reaction rate of $O + CH_4 \rightarrow OH + CH_3$ is negligible [28]. CH_3 in the first reaction mostly comes from the electron dissociation reaction and the reactions with electronically excited nitrogen. Combining the discharge temperature and the atomic-oxygen measurement here, we believe that the re-ignition results from a temperature increase (still below the auto-ignition temperature) and the kinetic enhancement from the discharge (e.g., the initiation of chain branching reactions) including reactions with increased atomic oxygen.

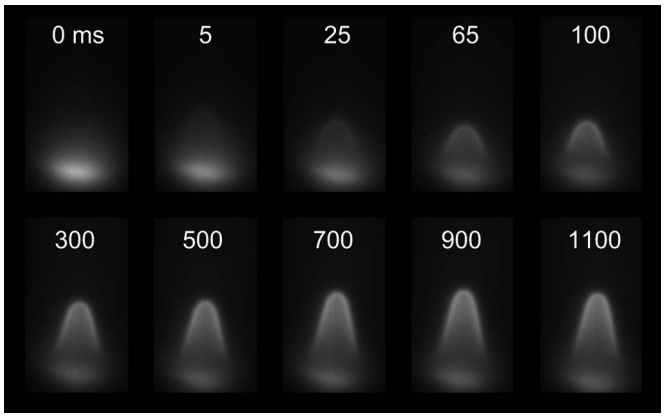

Fig. 7. Set of images for the re-ignition process at 20 W with a re-introduced total flow rate of 100 SCCM with an equivalence ratio of 1.1.

To investigate the temporal evolution of flame initiation and stabilization during the re-ignition, a high-speed camera was used. Fig. 7 shows a series of images for this re-ignition process at 20 W with a re-introduced reactant flow rate of 100 SCCM for methane and oxygen with an equivalence ratio of 1.1. The number on the top of each image is the time, in milliseconds, starting at the onset of emission from oxidation reactions. The images were taken at a repetitive rate of 10 000 Hz with an exposure time of 50 μs. In a very short time after the first image, a faint "ghost" flame quickly forms and then evolves to a smaller structure as the flame speed grows and the flame is stabilized. This effect is due to the initial breakdown of methane by the discharge; the microwave discharge is able to ignite the mixture, but it has yet to fully couple with the plasma. After 25 ms, the plasma energy starts to couple into the flame, which leads to a larger flame structure and to the reduction of the glow from the plasma discharge. The flame continues to grow in size, and the total time for full stabilization in Fig. 7 is about 900 ms. Experiments with different microwave powers have yielded similar results, and the stabilization time for the microwave power between 10 and 30 W is summarized in Table I. As expected, the stabilization time becomes smaller with higher microwave power as the higher discharge power and more radical concentration stabilize the ignition process faster. Our observations show that results at higher flow rates reveal that the initial "ghost" flame has no time to stabilize and cannot therefore anchor itself long enough to draw in the plasma energy for re-ignition to occur. In summary, the results show that the re-ignition occurs below the auto-ignition temperature and is a two-step process of initiating a fast pyrolysis flame,

TABLE I
MICROWAVE DISCHARGE PARAMETERS FOR POWERS BETWEEN 0 AND 30 W

Microwave Power	W	0	5	10	15	20	25	30
Microwave Air Discharge Volume	mm^3	0	0	35.8	68.2	106.75	214.2	387.1
N_2 rotational temperature	K	n/a	n/a	515	535	580	665	765
Thermocouple Temperature	K	n/a	n/a	618	643	681	713	733
Stabilization Time	ms	n/a	n/a	1,000	940	900	870	850

which, in turn, initiates the direct coupling of the plasma energy for full re-ignition to occur.

IV. CONCLUSION

LIF (OH, CO, and O), emission measurements, and high-speed photography have been used to characterize the re-ignition process in an efficient direct-coupled microwave-plasma-enhanced combustion system. A three-stage coupling process has been found for different levels of microwave power input, and the direct coupling concept can lead to higher flammability limits and flame speed. The OH concentration reaches and stays highest in Stage III, whereas CO, O concentration, and OH rotational temperature increase throughout all stages. In Stage III (microwave power exceeds 10 W), re-ignition is achieved when methane/oxygen is re-introduced into an atmospheric-pressure plasma discharge after cutting off the gas flow to extinguish the flame in a re-entrant microwave-plasma applicator system. Experiments show that, for re-ignition to occur, the electric field must be strong enough to fully establish a weakly ionized and self-sustained plasma discharge (Stage III), with elevated radical concentrations, before the ignition kernel is extinguished. The re-ignition can occur at gas flow speeds several times higher than typical flame propagation rates. Temperature measurements using both thermocouple measurements and rotational N_2 thermometry from spectrally resolved emission spectroscopy have been used. These measurements also reveal that re-ignition occurs below auto-ignition temperatures. High-speed imaging of the flame propagation of the whole phenomenon shows that this is a two-step process of initiating a light fast pyrolysis flame, which, in turn, starts the direct coupling process of the plasma energy into the flame for full re-ignition to occur and stabilize.

REFERENCES

[1] S. M. Starikovskaia, "Plasma assisted ignition and combustion," *J. Phys. D, Appl. Phys.*, vol. 39, no. 16, pp. R265–R299, Aug. 2006.

[2] A. Y. Starikovskii, "Plasma supported combustion," *Proc. Combustion Instit.*, vol. 30, no. 2, pp. 2405–2417, Jan. 2005.

[3] S. B. Leonov and D. A. Yarantsev, "Plasma-induced ignition and plasma-assisted combustion in high-speed flow," *Plasma Sources Sci. Technol.*, vol. 16, no. 1, pp. 132–138, Feb. 2007.

[4] W. Kim, H. Do, M. G. Mungal, and M. A. Cappelli, "Plasma-discharge stabilization of jet diffusion flames," *IEEE Trans. Plasma Sci.*, vol. 34, no. 6, pp. 2545–2551, Dec. 2006.

[5] D. H. Lee, K. T. Kim, M. S. Cha, and Y. H. Song, "Optimization scheme of a rotating gliding arc reactor for partial oxidation of methane," *Proc. Combustion Inst.*, vol. 31, no. 2, pp. 3343–3351, Jan. 2007.

[6] L. Bromberg, D. R. Cohn, A. Rabinovitch, and J. Heywood, "Emissions reductions using hydrogen from plasmatron fuel converters," *Int. J. Hydrogen Energy*, vol. 26, no. 10, pp. 1115–1121, Oct. 2001.

[7] T. Ombrello, X. Qin, Y. Ju, A. Gutsol, A. Fridman, and C. Carter, "Combustion enhancement via stabilized piecewise nonequilibrium gliding arc plasma discharge," *AIAA J.*, vol. 44, no. 1, pp. 142–150, Jan. 2006.

[8] A. B. Leonov, D. A. Yarantsev, A. P. Napartovich, and I. V. Kochetov, "Plasma-assisted ignition and flameholding in high-speed flow," presented at the 44th AIAA Aerospace Sciences Meeting, Reno, NV, 2006, AIAA-2006-563.

[9] A. Y. Starikovskii, N. B. Anikin, I. N. Kosarev, E. I. Mintoussov, M. M. Nudnova, A. E. Rakitin, D. V. Roupassov, S. M. Starikovskaia, and V. P. Zhukov, "Nanosecond-pulsed discharge for plasma-assisted combustion and aerodynamics," *J. Propulsion Power*, vol. 24, no. 6, pp. 1182–1197, 2008.

[10] G. Lou, A. Bao, M. Nishihara, S. Keshav, Y. G. Utkin, J. W. Rich, W. R. Lempert, and I. V. Adamovich, "Ignition of premixed hydrocarbon-air flows by repetitively pulsed, nanosecond pulse duration plasma," *Proc. Combustion Inst.*, vol. 31, no. 2, pp. 3327–3334, Jan. 2007.

[11] N. Chintala, A. Bao, G. Lou, and I. V. Adamovich, "Measurements of combustion efficiency in nonequilibrium RF plasma-ignited flows," *Combustion Flame*, vol. 144, no. 4, pp. 744–756, Mar. 2006.

[12] Y. D. Korolev and I. B. Matveev, "Nonsteady-state processes in a plasma pilot for ignition and flame control," *IEEE Trans. Plasma Sci.*, vol. 34, no. 6, pp. 2507–2513, Dec. 2006.

[13] L. Bromberg, D. R. Cohn, A. Rabinovitch, and J. Heywood, "Emissions reductions using hydrogen from plasmatron fuel converters," *Int. J. Hydrogen Energy*, vol. 26, no. 10, pp. 1115–1121, Oct. 2001.

[14] S. H. Zaidi, E. Stockman, X. Qin, Z. Zhao, S. Macheret, Y. Ju, R. B. Miles, D. J. Sullivan, and J. F. Kline, "Measurements of hydrocarbon flame speed enhancement in high-Q microwave cavity," presented at the 44th AIAA Aerospace Sciences Meeting Exhibit, Reno, NV, 2006, AIAA-2006-1217.

[15] E. S. Stockman, S. H. Zaidi, R. B. Miles, C. D. Carter, and M. D. Ryan, "Measurements of combustion properties in a microwave enhanced flame," *Combustion Flame*, vol. 156, no. 7, pp. 1453–1461, Jul. 2009.

[16] X. Rao, S. Hammack, C. Carter, I. Matveev, and T. Lee, "Combustion dynamics of plasma enhanced premixed and non-premixed flames," *IEEE Trans. Plasma Sci.*, vol. 38, no. 12, pp. 3265–3271, Dec. 2010.

[17] X. Rao, I. Matveev, and T. Lee, "Nitric oxide formation in a premixed flame with high level plasma energy coupling," *IEEE Trans. Plasma Sci.*, vol. 37, no. 12, pp. 2303–2313, Dec. 2009.

[18] A. Tropina, M. Uddi, and Y. Ju, "On the effect of nonequilibrium plasma on the minimum ignition energy—Part 1: Discharge model," *IEEE Trans. Plasma Sci.*, vol. 39, no. 1, pp. 615–623, Jan. 2011.

[19] T. Ombrello, Y. Ju, and A. Fridman, "Kinetic ignition enhancement of diffusion flames by nonequilibrium magnetic gliding arc plasma," *AIAA J.*, vol. 46, no. 10, pp. 2424–2433, Oct. 2008.

[20] N. Chintala, R. Meyer, A. Hicks, A. Bao, J. W. Rich, W. R. Lempert, and I. V. Adamovich, "Non-thermal ignition of premixed hydrocarbon-air flows by nonequilibrium rf plasma," *J. Propulsion Power*, vol. 21, no. 4, pp. 583–590, Jul./Aug. 2005.

[21] A. Y. Starikovskii, "Plasma supported combustion," *Proc. Combustion Inst.*, vol. 30, no. 2, pp. 2405–2417, Jan. 2005.

[22] L. Wu, J. Lane, N. P. Cernansky, D. L. Miller, A. A. Fridman, and A. Y. Starikovskii, "Plasma-assisted ignition below self-ignition threshold in methane, ethane, propane and butane–air mixtures," *Proc. Combustion Inst.*, vol. 33, no. 2, pp. 3219–3224, 2011.

[23] X. Rao, K. Hemawan, I. Wichman, C. Carter, T. Grotjohn, J. Asmussen, and T. Lee, "Combustion dynamics for energetically enhanced flames using direct microwave energy coupling," *Proc. Combustion Inst.*, vol. 33, no. 2, pp. 3233–3240, 2011.

[24] K. W. Hemawan, I. S. Wichman, T. Lee, T. A. Grojohn, and J. Asmussen, "Compact microwave reentrant cavity applicator for plasma assisted combustion," *Rev. Sci. Inst.*, vol. 80, no. 5, p. 053 507, May 2009.

[25] K. Kohse-Hoinghaus and J. B. Jeffries, *Applied Combustion Diagnostics*. New York: Taylor & Francis, 2002.

[26] J. M. Seitzman, J. Haumann, and R. K. Hanson, "Quantitative two photon LIF imaging of carbon monoxide in combustion gases," *Appl. Opt.*, vol. 26, no. 14, pp. 2892–2899, Jul. 1987.

[27] A. Mokhov, H. Levinsky, C. van der Meij, and R. Jacobs, "Analysis of laser-induced-fluorescence carbon monoxide measurements in turbulent nonpremixed flames," *Appl. Opt.*, vol. 34, no. 30, pp. 7074–7082, Oct. 1995.

[28] M. Uddi, N. Jiang, E. Mintusov, I. V. Adamovich, and W. R. Lempert, "Atomic oxygen measurements in air and air/fuel nanosecond pulse discharge by two photon laser induced fluorescence," *Proc. Combustion Inst.*, vol. 32, no. 1, pp. 929–936, 2009.
[29] J. Happold, P. Lindner, and B. Roth, "Spatially resolved temperature measurements in an atmospheric plasma touch using the A^2, $v = 0 > X2$, $v'' = 0$ OH band," *J. Phys. D, Appl. Phys.*, vol. 39, pp. 3615–3620, 2006.
[30] G. Faure and S. Shkol'Nik, "Determination of rotational and vibrational temperatures in a discharge with liquid non-metallic electrodes in air at atmospheric pressure," *J. Phys. D, Appl. Phys.*, vol. 31, p. 1212, 1998.
[31] R. Ono and T. Oda, "OH radical measurement in a pulsed arc discharge plasma observed by a LIF method," *IEEE Trans. Ind. Appl.*, vol. 37, no. 3, pp. 709–714, May/Jun. 2001.
[32] GRI-Mech 3.0. [Online]. Available: http://www.me.berkeley.edu/gri_mech/version30.
[33] N. L. Aleksandrov, S. V. Kindysheva, E. N. Kukaev, S. M. Starikovskaya, and A. Y. Starikovskii, "Simulation of the ignition of a methane–air mixture by a high-voltage nanosecond discharge," *Plasma Phys. Rep.*, vol. 35, no. 10, pp. 867–882, Oct. 2009.
[34] K. Becker, U. Kogelschatz, K. Schoenbach, and R. Barker, *Non-Equilibrium Air Plasmas at Atmospheric Pressure*. London, U.K.: Inst. Phys., 2005.
[35] C. Robinson and D. B. Smith, "The auto-ignition temperature of methane," *J. Hazardous Mater.*, vol. 8, no. 3, pp. 199–203, 1984.

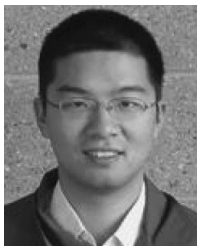

Xing Rao [redacted]. He received the B.S. degree in mechanical engineering and the M.S. degree in nuclear engineering from Tsinghua University, Beijing, China, in 2005 and 2007, respectively, and the Ph.D. degree in mechanical engineering from Michigan State University, East Lansing, in 2010.

He is currently a Particle Accelerator Mechanical Engineer with the Facility for Rare Isotope Beams, Michigan State University.

Stephen Hammack [redacted] He received the B.S. degree in mechanical engineering in 2009 from Michigan State University, East Lansing, where he is currently working toward the Ph.D. degree.

He is also currently a Graduate Research Assistant with Michigan State University. His research interests include laser diagnostics of combustion and plasma-assisted combustion.

Mr. Hammack is a Student Member of the American Institute of Aeronautics and Astronautics.

Campbell Carter [redacted] He received the B.S. degree in mechanical engineering from the University of Texas, Austin, and the Ph.D. degree in mechanical engineering from Purdue University, West Lafayette, IN.

Upon leaving Purdue University, he was a Postdoctoral Fellow with the Combustion Research Facility, Sandia National Laboratories, where he worked with Dr. R. Barlow on making simultaneous measurements of major and minor combustion species in turbulent flames. He joined the Systems Research Laboratories in 1993 and then Innovative Scientific Solutions, Inc., in 1997, developing and applying laser diagnostic techniques for the advanced propulsion group with the U.S. Air Force Research Laboratory (AFRL), Wright-Patterson AFB, OH. Since 2002, he has been directly working with the AFRL. His area of focus has been the development and the application of advanced laser diagnostics to harsh flow fields.

Dr. Carter is an active member of the combustion and combustion diagnostics communities and is a Fellow of the American Society of Mechanical Engineering and an Associate Fellow of the American Institute of Aeronautics and Astronautics.

Timothy Grotjohn received the undergraduate and Master's degrees in electrical engineering at the University of Minnesota, Minneapolis, in 1982 and 1984, respectively, and the Ph.D. degree in electrical engineering at Purdue University, West Lafayette, IN, in 1986.

He has been a Faculty Member of the Department of Electrical Engineering at Michigan State University (MSU), East Lansing, since 1987. He has been the Chairperson of the Department of Electrical and Computer Engineering at MSU, since 2005. His scholarly interests include the modeling, design, diagnostics, and applications of plasma-assisted materials processes and processing machines. A strong focus of his work is the use of models, including electromagnetic, plasma dynamic, and plasma chemistry models, for the design and control of microwave plasma reactors used for materials processing. In coordination with the modeling studies are plasma diagnostic studies. Recent work is especially looking at mini- and micro-scale plasma discharges and their application.

Dr. Grotjohn was the co-chair of the 2006 IEEE International Conference on Plasma Science that was held in Traverse City, Michigan.

Jes Asmussen, Jr. (S'66–M'67–SM'88–F'92–LF'04) received the B.S., M.S., and Ph.D. degrees in electrical engineering from the University of Wisconsin, Madison, in 1960, 1964, and 1967, respectively.

In 1967, he joined the Electrical and Computer Engineering Department at Michigan State University, East Lansing, where he served as Department Chairperson, from 1989 to 2000. He is currently a University Distinguished Professor and The Richard M. Hong Chaired Professor of Electrical Engineering and also serves as the Executive Director of the Fraunhofer USA Center for Coatings and Laser Applications.

Dr. Asmussen was the Conference Chairperson of the 33rd IEEE International Conference on Plasma Science that was held in Traverse City, Michigan in 2006.

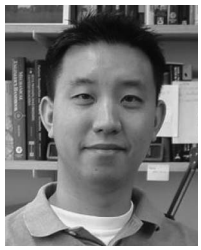

Tonghun Lee [redacted]. He received the B.S. degree in mechanical engineering from Yonsei University, Seoul, Korea, in 2000, and the M.S. and Ph.D. degrees in mechanical engineering from Stanford University, Stanford, CA, in 2002 and 2006, respectively.

He is current an Associate Professor in the Department of Mechanical Engineering at Michigan State University, East Lansing. His research interests include laser diagnostics of high-pressure combustion systems, plasma enhanced flames, as well as oxidation of novel biofuels. His research group at Michigan State University is devoted to fundamental research in applying laser based optical methods for development of advanced combustion and propulsion system technologies.